Journal of Magnetism and Magnetic Materials 442 (2017) 460–467

Contents lists available at ScienceDirect

Journal of Magnetism and Magnetic Materials

journal homepage: www.elsevier.com/locate/jmmm

Research articles

Structural, transport, magnetic, magnetocaloric properties and critical analysis of Ni-Co-Mn-Ga Heusler alloys

S. Arumugam [a,*], U. Devarajan [a], S. Esakki Muthu [a,b], Sanjay Singh [c], R. Thiyagarajan [d], M. Manivel Raja [e], N.V. Rama Rao [e], Alok Banerjee [f]

[a] Centre for High Pressure Research, School of Physics, Bharathidasan University, Tiruchirappalli, India
[b] Department of Physics, Karpagam College of Engineering, Coimbatore 641032, India
[c] Max Planck Institute for Chemical Physics of Solids, Nöthnitzer Strasse 40, D-01187 Dresden, Germany
[d] Centre for High Pressure Science and Technology Advanced Research (HPSTAR), Pudong, Shanghai 201203, China
[e] Advanced Magnetic Group, Defence Metallurgical Research Laboratory, Hyderabad, India
[f] Magnetism Laboratory, UGC-DAE-CSR, Indore, India

ARTICLE INFO

Article history:
Received 3 March 2017
Received in revised form 20 June 2017
Accepted 5 July 2017
Available online 8 July 2017

Keywords:
Ni-Co-Mn-Ga alloy
Magnetocaloric effect
Critical exponents
Mean field theory

ABSTRACT

In this work, we have investigated structural, transport, magnetic, magnetocaloric (MC) properties and critical exponents analysis of the $(Ni_{2.1-x}Co_x)Mn_{0.9}Ga$ ($x = 0$, 0.04, 0.12 and 0.2) Heusler alloys. For all compositions, cubic austenite (A) phase with metallic character is observed at room temperature (RT). With increasing of Co content, magnitude of resistivity decreases, whereas residual resistivity (ρ_0) and electron scattering factor (A) increases linearly. Magnetic measurements exhibit that ferromagnetic (FM) Curie temperature (T_C^A) increases towards RT by increasing Co concentration. All samples show conventional MC and maximum magnetic entropy change (ΔS_M^{peak}) of -2.8 Jkg^{-1} K^{-1} is observed for $x = 0.12$ at 147 K under 5 T. Further, hysteresis is observed between cooling and warming cycles around FM-PM (T_C^A) transition in $x = 0$, 0.04 samples, which suggests that first order nature of transition. However, there is no hysteresis across T_C^A for $x = 0.12$ and 0.2 samples suggesting second-order nature of the transition. The critical exponents are calculated for $x = 0.12$ sample around T_C^A using Arrott plot and Kouvel-Fisher method, the estimated critical exponents are found closer to the mean-field model reveals the long range ferromagnetic ordering in this composition.

1. Introduction

The family of Ni-Mn based Heusler alloys afford an extensive playground of interesting physical properties. The novel properties of Ni-Mn-Ga alloys have attracted a lot of attention in magneto-strain owing to their prospective applications in sensors and actuators [1,2]. The phase transformation [3] displayed in these alloys give rise to thermos-elasticity, shape memory effect (SME) [4–6], magneto resistance (MR) [7–10] and magnetocaloric (MC) [11–16].

Heusler alloys exhibits two transformations. A pure magnetic transition from paramagnetic (PM) to ferromagnetic (FM) within the cubic austensite phase and a structural transition from cubic austenite to low symmetry martensite phase. The martensite phase can be FM (or) antiferromagnetic (AFM)/PM depending on the alloy composition [4,6,17–19]. In the recent decade, the effect of compositional changes in Ni-Mn-Ga alloys by doping different elements have been studied intensively by experiment and theory [20–25]. Doping of magnetic elements in Heusler alloys exhibit trivial changes in physical properties. Curie and martensitic transitions (T_C and T_M) are altered by replacing various elements in X site of Ni-Mn-X (X = Al, Ga, In, Sn and Sb) system [26], T_C can be controlled by substitution of Co at Ni site of $(Ni_{53.25-x}Co_x)Mn_{21}Ga_{25}$ ($x = 0.75$, 1.5, 2.25) alloys [27].

We discuss about doping of magnetic elements at different sites of Ni-Mn-Ga system as follows: Doping of Co element at Ni site affects the critical temperatures and exchange interactions of martensite and austenite phases in $Ni_{50}Mn_{30}Ga_{20}$ alloy [28]. Fe doping at Mn site of $Ni_{48.7}Mn_{28.1}Fe_2Ga_{21.2}$ improves the magnetostriction and fracture toughness without change in its magnetic and thermos-elastic properties [29,30]. Doping of magnetic elements in Ni-Mn-Ga system at Ni site is expected to give more interesting phenomenon than other sites.

Inter-martensitic transformation is absent by substituting Co at Ni site in $Ni_{46.9}Co_{3.3}Mn_{28.8}Ga_{21}$ system due to local spins inversion of Co [31]. The structural stability and alteration of transformation

* Corresponding author.
E-mail address: sarumugam1963@yahoo.com (S. Arumugam).

http://dx.doi.org/10.1016/j.jmmm.2017.07.016
0304-8853/

temperatures (T_M and T_C) causes the change in electron density at Fermi level by interchanging of Co at Ni site of $(Ni_{2.16-x}Co_x)Mn_{0.84}$ Ga (x = 0.03–0.09) system [32]. In the $Ni_{50-x}Co_xMn_{50-y}Ga_y$ ($7 \leq x \leq 13$, $18 \leq y \leq 20$) system, Yu et al. [33] reports that partial substitution of Co for Ni atoms tuned the magnetic ordering of parent phase from AFM to FM and decreases T_M while increases T_C. The phase diagram of T_M and T_C in the $(Ni_{2.19-x}Fe_x)Mn_{0.81}$ Ga (x = 0–0.04) system reveals that T_M decreases gradually whereas T_C increase with Fe concentration [34]. Soto-parra et al. [21] clearly pointed out the electron per atom ratio (e/a) variation of T_M and T_C with Co content at Ni site of $(Ni_{50.8-x}Co_x)Mn_{24.8}Ga_{24.4}$ (x = 0–5.2) and Fe doped at Ni site of $(Ni_{52.7-x}Fe_x)Mn_{21.9}Ga_{25.4}$ (x = 0–5.3). The doping of both Co and Fe in these system reveals that T_M decreases whereas T_C increases with e/a. The magnetic field induced reverse phase transformations from AFM (or PM) martensite to FM austenite phase appear near RT in $Ni_{45}Co_5Mn_{36.7}In_{13.3}$ [4]. A steep increase (decrease) of thermal expansion is observed in $Ni_{41}Co_9Mn_{31.5}Ga_{18.5}$ due to martensitic (reverse martensitic) transition [35].

On the other hand, Co substitution at Mn site of $Ni_{47}Mn_{31}X_1$-Ga_{21} (X = Co, Fe) has strong effect on T_C and T_M, while for substitution of Fe at Mn site shows opposite effect in the same system [36]. The change in transformations temperatures (T_M and T_C) causes the change in electron density at the Fermi level by interchanging Mn site in $Ni_{2.16}(Mn_{0.84-y}Co_y)Ga$ (y = 0.04–0.14) system [32]. When the Co is doped in Ga site of $(Ni_{50.26}Mn_{27.30}Ga_{22.44})_{100-x}Co_x$ (x = 0–6), the phase transformation temperatures and crystal structures of martensitic phase is altered and Curie temperature of martensitic phase is lower than that of austenitic phase [37].

From the structural measurements, Satish Kumar et al. [31] observed that Co doped in Ni site of $Ni_{46.9}Mn_{28.8}Ga_{21}Co_{3.3}$ stabilizes cubic austenite structure at RT and martensite at low temperatures (230 and 180 K). On the other hand doping in Mn site of $Ni_{49.8}$-$Mn_{27.2}Ga_{21.2}Co_{1.8}$ non-modulated tetragonal and *7M* orthorhombic phase observed at 290 and 200 K, respectively. When Fe replaces Ga in $Ni_{50}Mn_{27}(Ga_{23-x}Fe_x)$ (x = 1,2) orthogonal structure is observed [36]. Cubic $L2_1$ structure is shown for Co doping in Ga and Mn site of $Ni_{48}Mn_{27}(Ga_{25-x}Co_x)$ (x = 1–4) and $Ni_{48}(Mn_{26-x}Co_x)$ Ga_{26} (x = 1–5) respectively [38]. X-ray diffraction patterns for the $Ni_{52.5}Mn_{20.1}Ga_{25.1}Fe_{2.3}$ [21] sample reveals martensite monoclinic *14M* and *10M* modulated structure at 145 and 270 K, respectively. X-ray diffraction patterns for $Ni_{48.7}(Mn_{30.1-x}Fe_x)Ga_{21.2}$ (x = 0–11) [39] depict that cubic austenite and tetragonal martensite phase coexist in x = 0 and 2, whereas only the cubic parent phase exists for remaining x = 5, 8 and 11 alloys. Martensite transformations are identified clearly from transport measurements for Co doped in Ga and Mn site of $Ni_{48}Mn_{27}(Ga_{25-x}Co_x)$ (x = 1–4) and $Ni_{48}(Mn_{26-x}Co_x)Ga_{26}$ (x = 1–5) alloys [38].

For some of the compositions change in magnetic entropy (ΔS_M) has been reported as follows: The melt spun ribbons of $Ni_{52}Mn_{26}$-Ga_{26} shows magneto-structural transition around 354 K with the increasing trend of MC (−15 to −30.3 $Jkg^{-1}K^{-1}$) for 2 and 5 Tesla fields [40]. Rama Rao et al. [41] reported near RT-MC (~309 K) for $Ni_{55}Mn_{20.6}Ga_{24.4}$ (−9.5 $Jkg^{-1}K^{-1}$) and $Ni_{55}Mn_{19.6}Ga_{25.4}$ (−10.4 $Jkg^{-1}K^{-1}$) ribbons. The $Ni_{2.15}Mn_{0.85}$ Ga and $Ni_{2.19}Mn_{0.81}$ Ga alloys shows an increasing trend of MC (−7.2 to −28 $JKg^{-1}K^{-1}$) [42]. All these literature survey reports suggest an importance of doping (especially Co) in various Heusler alloy system.

The first and second order phase transitions of Ni-Mn-In-Si alloys have been correlated through magnetic entropy and magnetoresistance [43]. Critical exponents are analysed near T_C in manganites [44] re-entrant metallic alloys like $Au_{0.81}Fe_{0.19}$, $Ni_{0.78}Mn_{0.22}$, $Ni_{0.79}Mn_{0.21}$, amorphous $Fe_{0.98}Zr_{0.08}$ [45] and Heusler alloys $Ni_{50}Mn_{35}In_{14}Si_1$ [46], $Mn_4Fe(Ge_{3-x}Si_x)$ [47], $Ni_{50}(Mn_{50-x}Sn_x)$ (x = 13,14) [48], Hence, the same analysis has been carried out to find the magnetism model theory. Moreover, Co addition in NiMnGa alloys provides an opportunity to control the Curie temperature of transforming phases (FM-Austenite to AFM/PM-Martensite).

The purpose of this work is to show how the doping of Co effectively improves structure, electron scattering, T_C, MC and critical behavior. To the best of our knowledge, no experimental study of the critical phenomena is reported in literature for the Co substitution in $(Ni_{2.1-x}Co_x)Mn_{0.9}$ Ga (x = 0–0.2) based system. However, the effect of Co doping increases the ΔS_M, Curie and martensitic temperatures due to effective magnetic moment (Co) ions at Ni site of Ni-Mn-Ga system. Among all samples, the x = 0.12 composition shows conventional MC with maximum ΔS_M of −2.8 $Jkg^{-1}K^{-1}$ near T_M region. Austenite structures are stabilized by varying Co (0–0.2) substitution and lowering the structural transition temperature. Further, critical behavior of x = 0.12 composition has been also studied, in which second order nature of FM-PM transition exists during magnetization measurement.

2. Experimental details

Ingots of $(Ni_{2.1-x}Co_x)Mn_{0.9}$ Ga (x = 0, 0.04, 0.12 and 0.2) alloys are prepared by melting the high purity starting elements (99.9% pure) in a vacuum arc melting furnace (procured from M/S. Vacuum Techniques Pvt. Ltd, Bangalore) under partial Argon atmosphere. The samples are re-melted four times to ensure homogeneity. These alloys are sealed and annealed under high vacuum at 1175 K for 24 h and then quenched. Elemental compositions are determined using scanning electron microscope (SEM, Leo 440*i*) attached with an X-ray energy dispersive spectroscope (EDS) setup. The structural analysis is carried out at RT using a Philips 3121 X-ray diffractometer with Cu-K_α radiation. The transport studies are carried out between 300–4 K using Closed Cycle Refrigerator with Variable Temperature Insert (CCR-VTI) from M/S.Cryo Industries of America, USA. The magnetization measurements are performed by means of a physical property measurement system (PPMS-9T) using vibrating sample magnetometer (VSM) module (Quantum Design, USA). The data are collected for all samples during field cooling and warming modes and isothermal magnetization data are measured at different temperatures around T_M and T_C regions. The transition temperatures such as T_C and T_M are obtained from deep point of corresponding derivative plots.

3. Results and discussion

The powder X-ray diffraction patterns are recorded at RT in $(Ni_{2.1-x}Co_x)Mn_{0.9}$ Ga (x = 0, 0.04, 0.12 and 0.2) which are shown in Fig. 1. The Bragg peaks for all samples indexed with cubic cell $L2_1$ structure with lattice parameter a = 5.8729, 5.8691, 5.8637 and 5.8618 Å for x = 0, 0.04, 0.12 and 0.2 samples, respectively. Only x = 0.12 composition has mixed martensite and austensite (M + A) phase at room temperature although the martensite transition temperature is below room temperature (147 K, Fig. 2a). The martensite phase at room temperature is stabilized due to the residual strains generated *via* grinding the ingot into powder. [49,50]. However, x = 0, 0.04 and 0.20 samples are retained in austensite phase at room temperature.

Fig. 2(a) shows the temperature dependent resistivity $\rho(T)$ curves for $(Ni_{2.1-x}Co_x)Mn_{0.9}$ Ga (x = 0–0.2) alloys. The small hump in resistivity is observed around 147 K and 165 K for x = 0.12 and 0.2 respectively which shows clear indication of martensite transition (T_M). The resistivity of all samples decreased with decreasing temperature. In general, resistivity of Heusler alloys can be influenced by electron-electron, electron-phonon and electron-magnon scattering mechanisms. However, the electron-phonon scattering contribution is relatively small in Heulser alloys at low

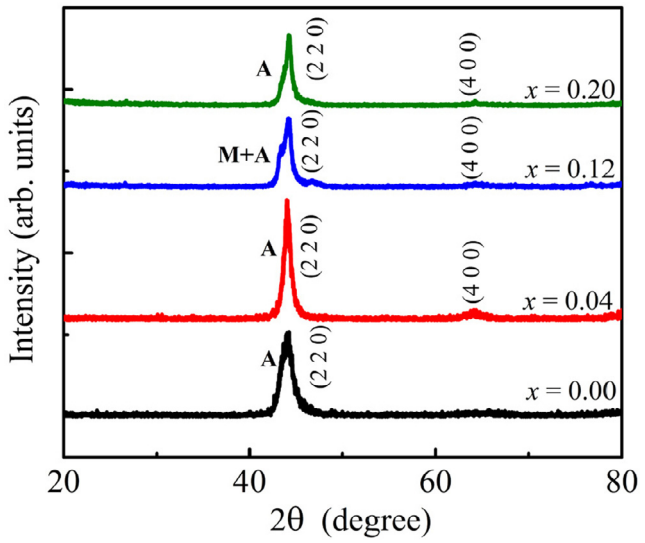

Fig. 1. XRD pattern of $Ni_{2.1-x}Co_xMn_{0.9}$ Ga (x = 0, 0.04, 0.12 and 0.2) alloys at room temperature.

temperature due to very low thermal fluctuation [51]. Hence, in our alloy system the electron-electron scattering is dominant at low temperature when compared to other scattering mechanisms. Therefore, power law equation is used to fit for all samples of $\rho(T)$

$$\rho = \rho_0 + AT^2 \quad (1)$$

where, ρ_0 is residual resistivity (due to the impurities or defects) and A is electron-electron scattering factor which depending on the slope of $\rho(T)$. The estimated values ρ_0 and A of are plotted as a function of Co doping as shown in the Fig. 2(b). It is clearly seen from the Fig. 2(b) that both the values are increased with Co concentration. The rate of decrease of resistivity with respect to temperature [i.e., dρ/dT] increases with Co doping throughout all the temperature range. i.e., the slope of curves increases with Co concentrations throughout all the temperature range. This is confirmed by the increasing of A value with Co doping [right axis of Fig. 2(b)]. This effect is due to the "substitution-induced" disorder by Co doping [52]. In the special case of x = 0, nominal upturn in the resistivity is observed at the low temperature range of 4–15 K. It is probably a localization effect due to Kondo effect or electron-electron interaction. But mostly in half metal Heusler alloys the low temperature minimum originates due to electron-electron interaction [53].

The temperature dependent magnetizations [$M(T)$] are measured in the range of 320–10 K during field cooled (FC) and field warming (FW) modes for $(Ni_{2.1-x}Co_x)Mn_{0.9}$ Ga (x = 0, 0.04, 0.12 and 0.2) alloys at constant magnetic field of 0.01 T which are shown in the Fig. 3(a–d). The x = 0 and 0.04 exhibit FM magneto-structural transition at 273 and 275 K respectively. Here, we have confirmed the first order transition by the presence of hysteresis between cooling and warming cycles [inset of Fig. 3(a) and (b)]. The decoupling of FM-PM and structural transition has been observed for x = 0.12 and 0.2 samples. The hysteresis around T_C is suppressed for these samples and suggested that presence of second order transition by increasing of Co content. The characteristic transformations temperatures of martensite transition (M_s, M_f, A_s and A_f) are indicated around the hysteresis region. On the other hand, an abrupt change in magnetization indicate Curie transitions (T_C^A) at 286.5 and 309 K for x = 0.12 and 0.2 samples respectively. The actual T_C^A is derived from the minima of the dM/dT vs T curves [shown in the inset of Fig. 3(c)]. Moreover, addition of Co brings T_C^A to higher values due to enhanced FM in the austenite phase. We found that T_C^A increases with the effect of Co doping in Ni site.

The $M(H)$ is measured around T_M region for x = 0 (between 260–310 K at 5 K interval), 0.04 (between 260–310 K at 5 K interval), x = 0.12 (110–170 K at 10 K interval) and x = 0.2 (110–180 K at 10 K interval), and it is shown in Fig. 4(a and b) during increasing and decreasing of magnetic field up to 5 T. It is found that magnetization decreases with increasing temperatures for x = 0 and x = 0.04 samples which are shown in Fig. 4(a and b). The magnetization is hard to saturate below 147 K (x = 0.12) and 165 K (x = 0.2) where these compositions are in martensite phase while this easily saturates above these temperatures because of austenite phase.

From these isothermal magnetization curves, the magneto entropy change (ΔS_M) is calculated for x = 0, 0.04, 0.12 and 0.2 samples around marternsitic region using Maxwell relation,

$$\Delta S_M = \int_0^H \left(\frac{\partial M(H,T)}{\partial T}\right)_H dH \quad (2)$$

The temperature dependence of magneto entropy change [$\Delta S_M(T)$] at different magnetic fields of 1, 3 and 5 T for $(Ni_{2.1-x}Co_x)Mn_{0.9}$ Ga (x = 0, 0.04, 0.12 and 0.2) alloys are shown in Fig. 5(a–d). The applied magnetic field increases the magnetic entropy change and the values are found to be negative corresponds to normal (conventional) MC. Further, the maximum ΔS_M values around T_M region are found to be −2.4, −2.34, −2.8 and −1.75 Jkg^{-1} K^{-1} at 5 T for x = 0, 0.04, 0.12 and 0.2 alloys respectively. In comparison with $Ni_{51.5}Mn_{22.7}Ga_{25.8}$ and $Ni_{49.5}Mn_{25.4}Ga_{25.1}$ which show ΔS_M of 4.1 Jkg^{-1} K^{-1} at 196 K in the field of 0.9 T and −11 Jkg^{-1} K^{-1} around 177 K at a field of 2 T respectively [11,12], the value of ΔS_M obtained in our system is lower, however it is higher than the ΔS_M (−2.2 Jkg^{-1} K^{-1} around 296 K at 5 T) value of $Ni_{50}CoMn_{36}Sn_{13}$ [54].

Furthermore, T_C and T_M variation of magnetic elements (Co, Fe) doped in NiMnGa compounds are presented in Fig. 6(a and b). In our present series Co is doped at Ni site of $(Ni_{2.1-x}Co_x)Mn_{0.9}$ Ga (x = 0–0.2) for which T_M decreases (273–164 K) and T_C increases

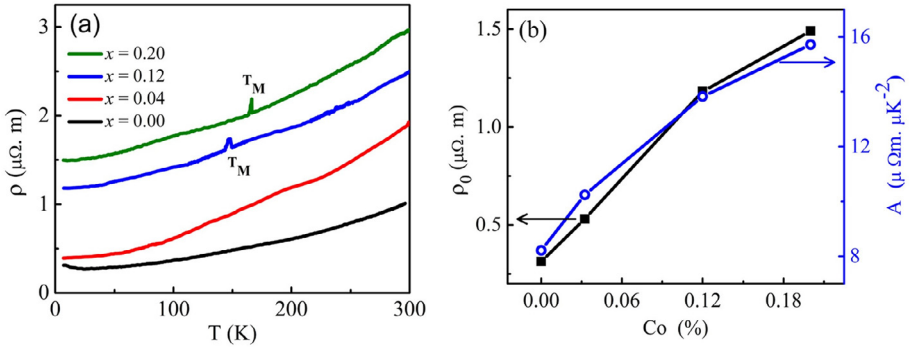

Fig. 2. Transport studies (a) ρ(T) of $Ni_{2.1-x}Co_xMn_{0.9}$ Ga (x = 0, 0.04, 0.12 and 0.2) alloys, (b) Co% variant residual resistivity (ρ_0) and electron-electron scattering factor (A).

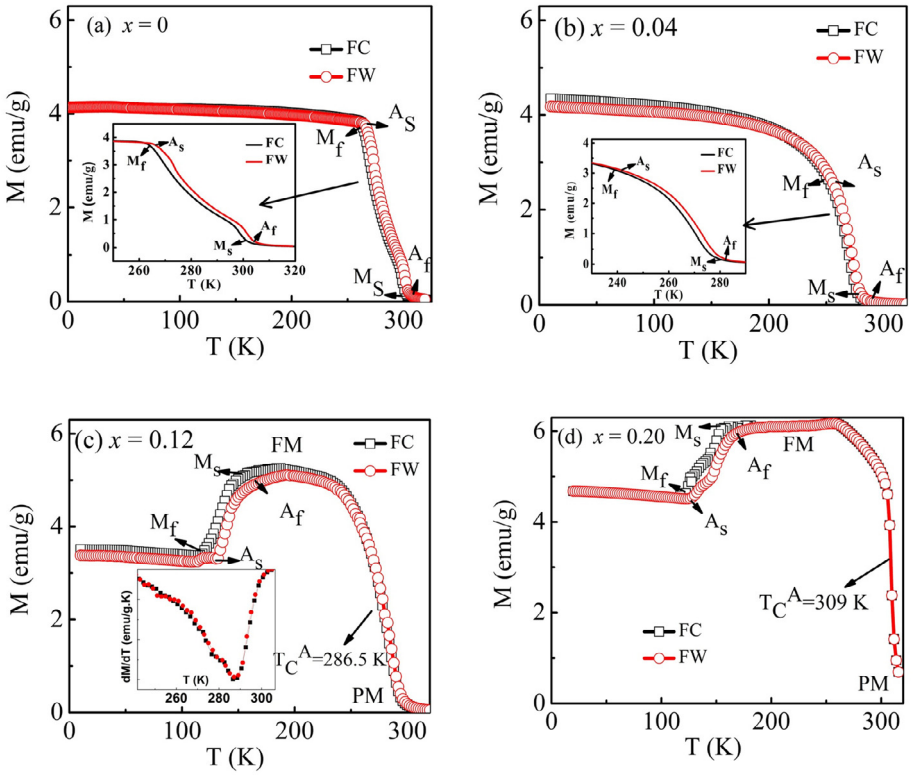

Fig. 3. Temperature dependent Magnetization of $Ni_{2.1-x}Co_xMn_{0.9}$ Ga, (a) $x = 0$ [inset: enlarged view of main plot in hysteresis region], (b) $x = 0.04$ [inset: enlarged view of main plot in hysteresis region], (c) $x = 0.12$ [derivative plots for main graphs to find T_C and also show suppression of hysteresis], (d) $x = 0.2$ alloys under 0.01 T.

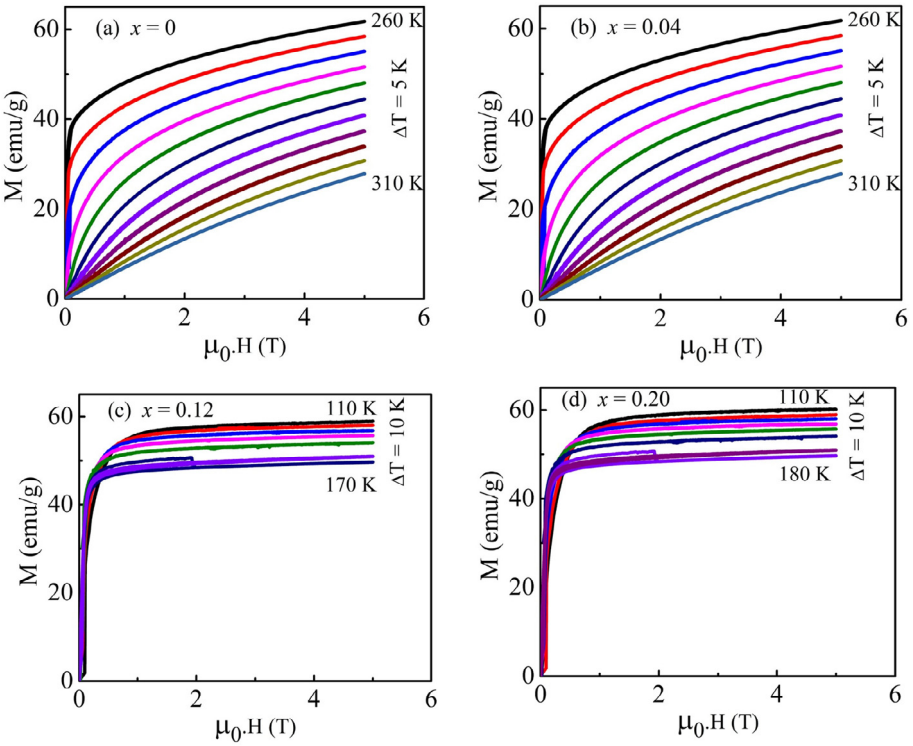

Fig. 4. (a–d) Isothermal curves at T_M of $Ni_{2.1-x}Co_xMn_{0.9}$ Ga ($x = 0$, 0.04, 0.12 and 0.2) alloys.

(284–309 K). Khovailo et al. [27] reports that T_M decreases (318–306 K) and T_C increases (348–367 K) in $(Ni_{2.16-x}Co_x)Mn_{0.84}$ Ga ($x = 0.03$–0.09) system, T_M decreases (317–223 K) and T_C increases (347–395 K) for $(Ni_{2.2-x}Fe_x)Mn_{0.8}$ Ga ($x = 0.04$–0.16). For another system $(Ni_{2.19-x}Fe_x)Mn_{0.81}$ Ga ($x = 0$–0.04), T_M decreases (340–285 K) and T_C slightly increases (340–345 K) [34].

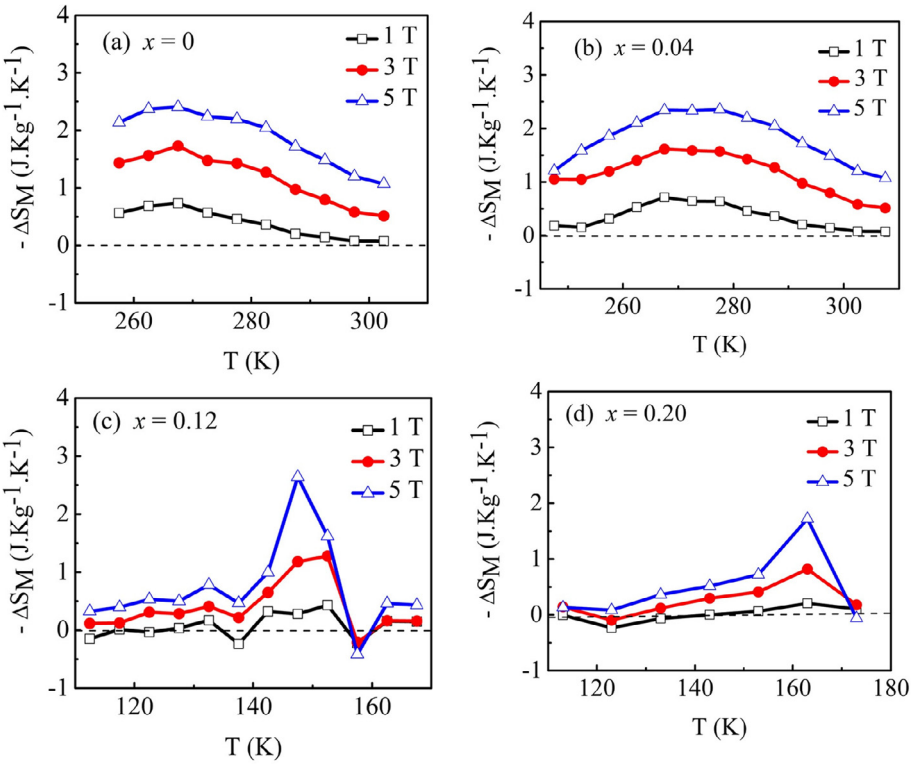

Fig. 5. (a–d) Temperature dependent magnetic entropy near T_M of $Ni_{2.1-x}Co_xMn_{0.9}$ Ga (x = 0, 0.04, 0.12 and 0.2) alloys.

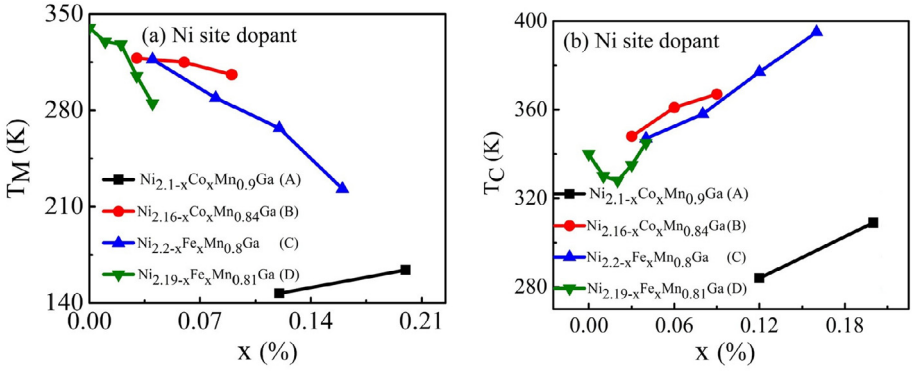

Fig. 6. (a and b) T_M and T_C variation of magnetic elements (Co, Fe) doped in Ni site of NiMnGa compounds; (A) $Ni_{2.1-x}Co_xMn_{0.9}$ Ga (x = 0, 0.04, 0. 12, 0.2), [present work], (B) $Ni_{2.16-x}Co_xMn_{0.84}$ Ga (x = 0.03, 0.06, 0.09) [Khovailo, et al. [27] JMMM (2004)], (C) $Ni_{2.2-x}Fe_xMn_{0.8}$ Ga (x = 0.04, 0.08, 0.12, 0.16) [27] (D) $Ni_{2.19-x}Fe_xMn_{0.81}$ Ga (x = 0, 0.01, 0.02, 0.03, 0.04) [Sokolovsiy *et al* [34], JMMM (2013)].

Generally, *e/a* ratio decreases with doping of magnetic elements at Ni site of NiMnGa systems. The *e/a* variation of doped (Co, Fe) magnetic elements at Ni site of NiMnGa and our system are shown in Fig. 7(a–c). Soto–parra et al. [21] reported that doping of Co in Ni site of $(Ni_{2.03}Co_x)Mn_{0.9}Ga_{0.97}$ (x = 0–0.2) and Fe in $(Ni_{2.108-x}Fe_x)Mn_{0.87}$ Ga (x = 0–0.21) decreases T_M and increases T_C follows the *e/a* variation. The *e/a* ratio can be correlated with the T_M where an increase (decrease) in *e/a* ratio increases (decreases) the value of T_M [55]. In our selected Co doping compounds, T_M decreases with increasing *e/a* ratio.

As discussed earlier, for the selected series of samples $((Ni_{2.1-x}Co_x)Mn_{0.9}$ Ga) a first order FM-PM transition is observed for x = 0 and 0.04, whereas second order FM-PM transition for x = 0.12 and 0.20. Hence, M (H) around FM region are also measured for x = 0.12 (275 to 330 K at 5 K interval) and x = 0.2 (240 to 320 K at 10 K interval) as shown in Fig. 8(a and b). As we expected, these samples do not show hysteresis, and hence confirms the presence of second order nature. Fig. 9(a) shows the Arrott plots around magnetic transition (T_C^A) for x = 0.12 around FM-PM transition in the austenite phase.

However, at low field region, small deviations from a straight line can occur in the Arrott plot due to misaligned magnetic domains. Hence, it has been removed to consider the sample as homogeneous for the analysis. Based on Banerjee criterion, the positive slopes are observed in all curves of Arrott plot reconfirms the presence of second-order phase transition. Moreover, second-order phase transitions, T_C can also be derived from M^3 vs H plot [57] and it is shown an inset of Fig. 9(a). In order to understand the FM nature of second order transition in x = 0.12 sample, the critical behavior is analysed using conventional iterative method through Arrott plot and Kouvel-Fisher plots [56,57] as follows:

The second order FM transition near the Curie points are characterized by a set of critical exponents' β (associated with the spontaneous magnetization M_S), γ (associated with the initial

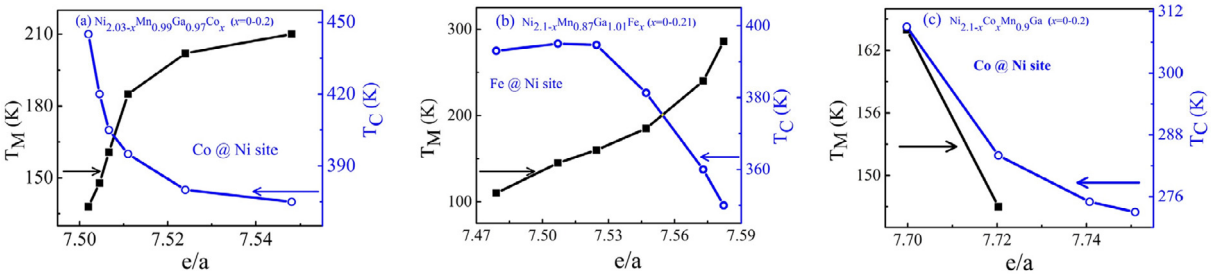

Fig. 7. (a–c) e/a variation of doped magnetic elements (Co, Fe) at Ni site of NiMnGa system.

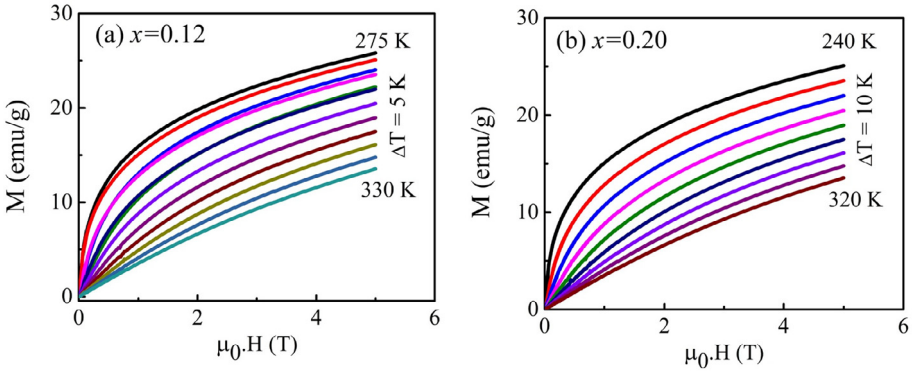

Fig. 8. (a and b) Isothermal curves near T_C of $Ni_{2.1-x}Co_xMn_{0.9}$ Ga ($x = 0.12$ and 0.2) alloys.

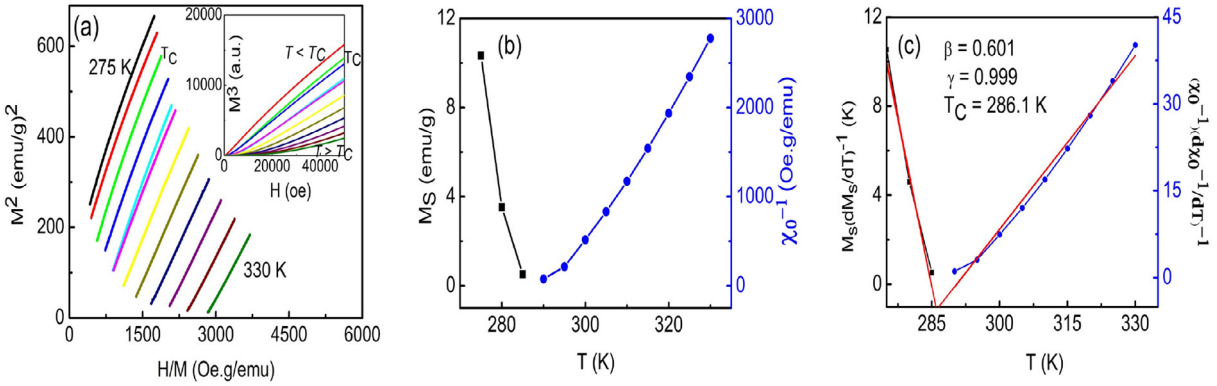

Fig. 9. (a) Arrott plot (b) Temperature dependence of spontaneous magnetization (M_S) and inverse initial susceptibility (χ_0^{-1}) (c) Kouvel- Fisher plots of $M_S(dM_S/dT)^{-1}$ and $\chi_0^{-1}(d\chi_0^{-1}/dT)^{-1}$ vs T (d) ln(M) vs ln(H) plot of $Ni_{2.1-x}Co_xMn_{0.9}$ Ga ($x = 0.12$) alloy.

susceptibility χ_0), and δ (associated with the critical magnetization isotherm at T_C). The mathematical definitions of the critical exponents from magnetization measurements are given as following relation:

$$M_S(0, T = M_0(-\varepsilon)^{\beta} \qquad \varepsilon < 0, T < T_C \tag{3}$$

$$\chi_0^{-1}(0, T) = (h_0/M_0)(\varepsilon)^{\gamma} \qquad \varepsilon > 0, T > T_C \tag{4}$$

$$M(H, T_C) = D(H)^{1/\delta} \qquad \varepsilon = 0, T = T_C \tag{5}$$

where, M_0, h_0/M_0 and D are the critical amplitudes. M_S, χ_0^{-1} and $\varepsilon = (T\text{-}T_C^A)/T_C^A$ are the spontaneous magnetization, initial inverse susceptibility and reduced temperature respectively, these parameters can be calculated from Fig. 9(b) and (c) as follows: the temperature at which the curve passes through the origin is T_C^A. The polynomial fitting of each curve and linear extrapolation above T_C^A yields M_S whereas below T_C^A yields χ_0^{-1}. The temperature dependence of M_S and χ_0^{-1} of $x = 0.12$ alloy is shown in Fig. 9(b).

The conventional way of Kouvel–Fisher method is used for the efficient and accurate determination of T_C^A and the critical exponents β, γ and δ Kouvel et al. [58]. The Eqs. (3)–(5) are modified as per Kouvel–Fisher method as

$$\frac{M_S(T)}{dM_S(T)/dT} = \frac{T - T_C}{\beta} \tag{6}$$

$$\frac{\chi_0^{-1}(T)}{d\chi_0^{-1}(T)/dT} = \frac{T - T_C}{\gamma} \tag{7}$$

$$\log M(H, T_C) = \frac{\log H}{\delta} \tag{8}$$

According to Eqs. (6) and (7), $M_S\,(dM_S/dT)^{-1}$ vs T and $\chi_0^{-1}(d\chi_0^{-1}/dT)^{-1}$ vs T should be a straight line with slopes $1/\beta$ and $1/\gamma$ should meet T axis corresponds to the T_C^A. Fig. 9(c) shows the Kouvel-Fisher

Table 1
Critical exponents values of $Ni_{2.1-x}Co_xMn_{0.9}$ Ga ($x = 0.12$) alloy.

x	T_M (K)	T_c (K)	Critical exponents			
			β	γ	δ	Order
0.12	147	286.5	0.601	0.999	2.55	Long range FM – Mean field theory

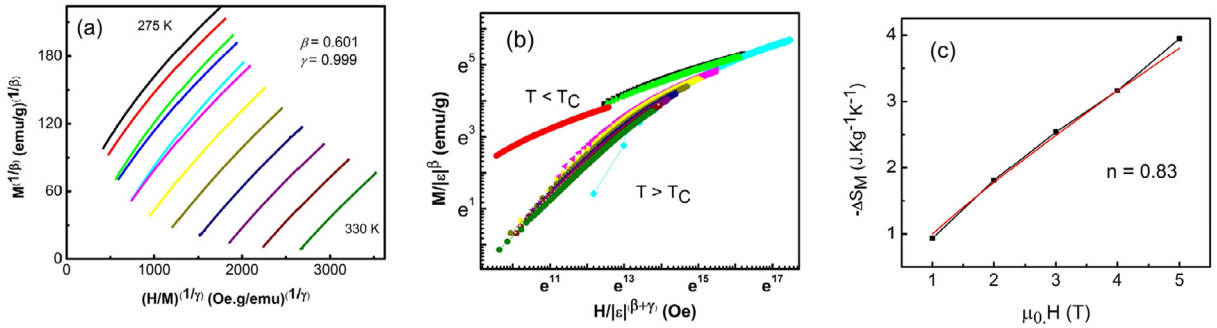

Fig. 10. (a) Modified Arrott plot using the equation of state; (b) Scaling plot on log–log scale indicating two universal curves below and above T_C; (c) Field dependence of the magnetic entropy change $-\Delta S_M$ for the $x = 0.12$ sample. The solid lines are fitted plot using universal curve to determine the value of n; (d) Normalized entropy change $\Delta S_M^{peak}/\Delta S_M$ vs rescaled temperature (θ) for different magnetic fields.

plots $[M_S(dM_S/dT)^{-1}$ vs T and $\chi_0^{-1}(d\chi_0^{-1}/dT)^{-1}$ vs $T]$ for $x = 0.12$ sample. The T_C^A for $x = 0.12$ sample obtained from these iterative method is 286.5 K which agrees with T_C^A derived from M (T) plots. The values of β and γ for $x = 0.12$ sample is calculated from the reciprocal of slopes from $M_S(dM_S/dT)^{-1}$ vs T and $\chi_0^{-1}(d\chi_0^{-1}/dT)^{-1}$ vs T plots respectively. The β *and* γ values are 0.601 and 0.999 for $x = 0.12$ sample and these values are shown in Table 1.One of the critical exponent δ which is associated with the critical magnetization isotherm at T_C^A is determined using Eq. (8). Fig. 9(d) shows ln M vs ln H plots at T_C^A of $x = 0.12$ sample. Based on the Eq. (8), the linear fit of each plot yields the value of $1/\delta$. The δ value is 2.55 for $x = 0.12$ sample. The reliability of the calculated values with Widom scaling relation $\gamma - \beta(\delta - 1) = 0$, the obtained values is 0.067 for $x = 0.12$ sample. Our critical exponents values are nearly match with the values of mean field theory ($\beta = 0.5$, $\gamma = 1.0$, $\delta = 3.0$) and it confirms that $x = 0.12$ exhibits long range ferromagnetic ordering. Thus, the increasing of Co content in $Ni_{2.1-x}Co_xMn_{0.9}$ Ga increases the long range ferromagnetic order around austenitic transition.

The estimated values of these critical exponents have been verified by Modified Arrott plot and scaling equation of state as follows:

$$\left(\frac{H}{M}\right)^{(1/\gamma)} = a\frac{(T - T_c)}{T} + bM^{(1/\beta)} \tag{9}$$

$$(M(H,\varepsilon) = (\varepsilon)^{\beta} f_{\pm}[H/\varepsilon^{(\gamma+\beta)}] \tag{10}$$

The modified Arrott and scaling equation plots are shown in Fig. 10(a and b) respectively. As clearly seen in Fig. 10(a), at higher fields, the isotherms introduce almost linear and parallel straight lines with values of $\beta = 0.601$ and $\gamma = 0.999$. Similarly, β and γ are tested by using the static-scaling hypothesis generalized in the Eq. (10) Where f_+ for $T > T_C$ and f_- for $T < T_C$ are regular functions. $M\varepsilon^{-\beta}$ as a function of $H\varepsilon^{-(\gamma+\beta)}$ is plotted in Fig. 10(b) by using the values of critical exponents. All magnetization data points fall on the universal branches of f_- for $T < T_C$ and of f_+ for $T > T_C$ are in good agreement with the descriptions of the scaling hypothesis. This also supports that values of critical exponents and T_C are accurate enough.

The MC data of different materials of same universality class should fall onto the same curve, irrespective of the applied magnetic field. The field dependence of ΔS_M is given by the following equation

$$\Delta S_M|_{T=Tc} \infty H^n \text{where} n = 1 + 1/\delta(1 - 1/\beta) \tag{11}$$

Thus, the value of n from Eq. (11) is 0.7505 using the values of $\beta = 0.601$ and $\gamma = 0.999$. The MC has been calculated around FM region of 0.12 sample, since Eq. (11) requires (not shown here). Based on Eq. (11), ΔS_M^{peak} vs H is plotted as show in Fig. 10(c), and value of n obtained from fitting of above equation is 0.83, which is nearly with that obtained from the critical exponents.

4. Conclusion

In summary, the partial substitution of Co in Ni site of $(Ni_{2.1-x}Co_x)Mn_{0.9}$ Ga ($x = 0$, 0.04, 0.12 and 0.2) alloys has been investigated through structural, transport, magnetic and magnetocaloric properties. For all the compositions, the $L2_1$ cubic structure is confirmed by powder XRD at RT. Transport measurement reveals that increase in the magnitude of ρ, residual resistivity (ρ_0) and electron scattering factor (A) with Co substitution. The magnetization measurements reveal that decoupling of austenitic and maternstic transition for $x = 0.12$ sample. The presence of martensite around FM transition in $x = 0$ and 0.04 samples exhibit first-order transition, whereas, appearance of austenite around FM transition leads second-order nature for $x = 0.12$ and 0.2 samples. The change in magnetic entropy (ΔS_M) is also calculated using Maxwell's relation for all four samples. The ΔS_M^{peak} is obtained (-2.8 Jkg^{-1} K^{-1}) for $x = 0.12$ sample. Further, critical behavior of $x = 0.12$ composition has been studied due to its second order nature of FM-PM transition. The estimated values of critical exponents suggested mean-field model, and hence suggested the presence of long-range ferromagnetic nature. The values are verified by modified Arrott plot, scaling equation of state using isothermal curves, where as ΔS_M^{peak} vs H plot and universal curve theory using MC values.

Acknowledgements

The authors acknowledge the DST (SERB, PURSE), BRNS-Mumbai, CEFIPRA-New Delhi, DRDO and UGC-RFSMS for their financial support. The authors would also like to acknowledge

Defence Metallurgical Research Laboratory (DMRL), Hyderabad for their support in carrying out sample preparation. The author R.T. acknowledges for the support of NSAF, China (Grant No.: U1530402). The author S.S thanks to Alexander von Humboldt foundation, Germany for research fellowship.

References

[1] S.J. Murray, M. Marioni, S.M. Allen, R.C. O'Handley, T.A. Lograsso, Appl. Phys. Lett. 77 (2000) 886.
[2] K. Ullakko, J.K. Huang, C. Kantner, R.C. O'Handley, V. Kokorin, Appl. Phys. Lett. 69 (1996) 1966.
[3] P.J. Webster, K.R.A. Ziebeck, S.L. Town, M.S. Peak, Philos. Mag. B 49 (1984) 295.
[4] R. Kainuma, Y. Imano, W. Ito, Y. Sutou, H. Morito, S. Okamoto, O. Kitakami, K. Oikawa, A. Fujita, T. Kanomata, K. Ishida, Nature (London) 439 (2006) 957.
[5] J. Pons, E. Cesari, C. Segui, F. Masdeu, R. Santamarta, Mater. Sci. Eng. A. 481–482 (2008) 57–65.
[6] A.N. Vasilev, A.D. Bozhko, V. Khovailo, I.E. Dikshtein, V.G. Shavrov, V.D. Buchelnikov, M. Matsumoto, S. Suzuki, T. Takagi, J. Tani, Phys. Rev. B 59 (1999) 1113.
[7] C. Biswas, R. Rawat, S.R. Barman, Appl. Phys. Lett. 86 (2005) 202508.
[8] K. Koyama, H. Okada, K. Watanabe, T. Kanomata, W. Ito, K. Oikawa, R. Kainuma, Appl. Phys. Lett. 89 (2006) 182510.
[9] V.K. Sharma, M.K. Chattopadhyay, K.H.B. Shaeb, A. Chouhan, S.B. Roy, Appl. Phys. Lett. 89 (2006) 222509.
[10] Sanjay Singh, R. Rawat, S. Esakki Muthu, S.W. D'Souza, E. Surad, A. Senyshyn, S. Banik, P. Rajput, S. Bhardwaj, A.M. Awasthi, Rajeev Ranjan, S. Arumugam, D.L. Schlagel, T.A. Lograsso, Aparna Chakrabarti, S.R. Barman, Phys. Rev. Lett. 109 (2012) 246601.
[11] F.X. Hu, B.G. Shen, J.R. Sun, Appl. Phys. Lett. 76 (2000) 3460.
[12] J. Marcos, A. Planes, L. Manosa, F. Casanova, X. Batlle, A. Labarta, B. Martınez, Phys. Rev. B 66 (2002) 224413.
[13] T. Krenke, E. Duman, M. Acet, E.F. Wassermann, X. Moya, L. Manosa, A. Planes, Nat. Mater. 4 (2005) 450.
[14] Z.D. Han, D.H. Wang, C.L. Zhang, S.L. Tang, B.X. Gu, Y.W. Du, Appl. Phys. Lett. 89 (2006) 182507.
[15] X. Moya, L. Manosa, A. Planes, S. Aksoy, T. Krenke, M. Acet, E.F. Wassermann, Phys. Rev. B. 75 (2007) 184412.
[16] Sanjay Singh, S. Esakki Muthu, A. Senyshyn, P. Rajput, E. Surad, S. Arumugam, S.R. Barman, Appl. Phys. lett. 104 (2014) 051905.
[17] M. Matsumoto, T. Takagi, J. Tani, T. Kanomata, N. Muramatsu, A.N. Vasil'ev, Mater. Sci. Eng. A 273 (1999) 326.
[18] S. Banik, Aparna Chakrabarti, U. Kumar, P.K. Mukhopadhyay, A.M. Awasthi, R. Ranjan, J. Schneider, B.L. Ahuja, S.R. Barman, Phys. Rev. B 74 (2006) 085110.
[19] Sanjay Singh, R. Rawat, S.R. Barman, Appl. Phys. Lett. 99 (2011) 021902.
[20] S.R. Barman, Aparna Chakrabarti, Sanjay Singh, S. Banik, S. Bhardwaj, P.L. Paulose, B.A. Chalke, A.K. Panda, A. Mitra, A.M. Awasthi, Phys. Rev. B 78 (2008) 134406.
[21] D.E. Soto-Parra, X. Moya, L. Manosa, A. Planes, H. Flores- Zuniga, F. Alvarado-Hernandez, R.A. Ochoa-Gamboa, J.A. Matutes-Aquino, D. Rios-Jara, Philos. Mag. 90 (2010) 2771.
[22] T. Hickel, M. Uijttewaal, A. Al-Zubi, B. Dutta, B. Grabowski, J. Neugebauer, Adv. Eng. Mater. 14 (2012) 547.
[23] Q.M. Hu, H.B. Luo, C.M. Li, L. Vitos, R. Yang, Sci. China Tech. Sci. 55 (2012) 295.
[24] P. Entel, M. Siewert, M.E. Gruner, H.C. Herper, D. Comtesse, R. Arroyave, N. Singh, A. Talapatra, V. Sokolovskiy, V.D. Buchelnikov, Eur. Phys. J. B 86 (2013) 65.
[25] Sanjay Singh, S.W. D'Souza, K. Mukherjee, P. Kushwaha, S.R. Barman, Agarwal Sandheep, P.K. Mukhopadhyay, Aparna Chakrabarti, E.V. Sambathkumaran, Appl. Phys. Lett. 104 (2014) 231909.
[26] T. Kanomato, K. Shirakawa, T. Kaneko, J. Magn. Magn. Mater. 65 (1987) 76–82.
[27] V. Khovailo, V.A. Chernenko, A. Cherechukin, T. Takagi, T. Abe, J. Magn. Magn. Mater. 272 (2004) 2067.
[28] F. Albertini, S. Fabbrici, A. Paoluzi, J. Kamarad, Z. Arnold, L. Righi, M. Solzi, G. Porcari, C. Pernechele, D. Serrate, P. Algarabel, Mater. Sci. Forum. 684 (2011) 151.
[29] A. Cherechukin, I.E. Dikshtein, D.I. Ermakova, A.V. Glebova, V. Koledova, D.A. Kosolapov, V.G. Shavrov, A. Tulaikova, E.P. Krasnoperov, T. Takagi, Phys. Lett. A 291 (2001) 175.
[30] H.B. Wang, F. Chen, Z.Y. Gao, W. Cai, L.C. Zhao, Mater. Sci. Eng. A 438–440 (2006) 990.
[31] A. Satish Kumar, M. Ramudu, V. Seshubai, Phase Trans. 85 (2012) 1045.
[32] V. Khovailo, T. Abe, V. Koledov, M. Matsumoto, H. Nakamura, R. Note, M. Ohtsuka, V.G. Shavrov, T. Takagi, Mater. Trans. 44 (2003) 2509.
[33] S. Yu, Y. Yu, Z.X. Cao, L. Ma, G.D. Liu, J.L. Chen, G.H. Wu, B. Zhang, X. Zhang, Appl. Phys. Lett. 91 (2007) 102507.
[34] V. Sokolovskiy, R. Fayzullin, V.D. Buchelnikov, M.O. Drobosyuk, S.V. Taskaev, V. Khovaylo, J. Magn. Magn. Mat. 343 (2013) 6–12.
[35] T. Sakon, K. Sasaki, D. Numakura, M. Abe, H. Nojiri, Y. Adachi, T. Kanomata, Mater. Trans. 54 (2013) 9–13.
[36] S. Guo, Y. Zhang, B. Quan, J. Li, Y. Qi, X. Wang, Smart Mater. Struct. 14 (2005) S236.
[37] V. Sanchez-Alarcos, J.I. Perez-Landazabal, V. Recarte, C. Gomez-Polo, J.A. Rodr guez Velamazan, Acta Mater. 56 (2008) 5370–5376.
[38] X.Q. Chen, X. Lu, D.Y. Wang, Z.X. Qin, Smart Mater. Struct. 17 (2008) 065030.
[39] F. Chen, H.B. Wang, Y.F. Zheng, W. Cai, L.C. Zhao, J. Mater. Sci. 40 (2005) 219–221.
[40] Z. Li, Y. Zhang, C.F. Sanchez-Valdes, J.L. Sanchez Llamazares, C. Esling, X. Zhao, L. Zuo, Appl. Phys. Lett. 104 (2014) 044101.
[41] N.V. Rama Rao, R. Gopalan, V. Chandrasekaran, K.G. Suresh, J. Alloys Compd. 478 (2009) 59.
[42] L. Pareti, M. Solzi, F. Albertini, A. Paoluzi, Eur. Phys. J. B 32 (2003) 303–307.
[43] I.D. Rodionov, D.E. Mettus, A.P. Kazakov, M.V. Prudnikova, V.N. Prudnikov, I.S. Dubenko, A.B. Granovsky, Phys. Solid State 55 (2013) 1861.
[44] R. Thiyagarajan, S. Esakki Muthu, S.K. Barik, R. Mahendiran, S. Arumugam, J. Appl. Phys. 113 (2013) 023904.
[45] M. Haetinger Cláudia, Luis. Ghivelder, Jacob Schaf, Paulo Pureur, J. Phys.: Condens. Matter. 21 (2009) 506006.
[46] R. Das, P. Alagarsamy, A. Srinivasan, EPL 108 (2014) 66004.
[47] M. Halder, S.M. Yusuf, A.K. Nigam, J. Appl. Phys. 110 (2011) 113915.
[48] Phan The-Long, P. Zhang, N.H. Dan, N.H. Yen, P.T. Thanh, T.D. Thanh, M.H. Phan, S.C. Yu, Appl. Phys. Lett. 101 (2012) 212403.
[49] Sanjay Singh, Pallavi Kushwaha, F. Scheibel, Peter Hanns, Liermann, S.R. Barman, M. Acet, C. Felser, Dhananjai Pandey, Phys. Rev. B 92 (2015) 020105.
[50] Sanjay Singh, M. Maniraj, S.W. D'Souza, R. Ranjan, S.R. Barman, Appl. Phys. Lett. 96 (2010) 081904.
[51] U. Devarajan, Sanjay Singh, S. Esakki Muthu, G. Kalai Selvan, P. Sivaprakash, S. Roy. Barman, S. Arumugam, Appl. Phys. Lett. 105 (2014) 252401.
[52] V. Ponnambalam, Paola N. Alboni, J. Edwards, Terry M. Tritt, Slade R. Culp, S. Joseph Poon, J. Appl. Phys. 103 (2008) 063716.
[53] M. Aftab, G. Hassnain Jaffari, S.K. Hasanain, Turab Ali Abbas, S. Ismat Shah, J. Appl. Phys. 114 (2013) 103903.
[54] Elias Palacios, Juan Bartolomé, Gaofeng Wang, Ramon Burriel, Konstantin Skokov, Sergey Taskaev, Vladimir Khovaylo, Entropy 17 (2015) 1236.
[55] T. Krenke, M. Acet, E.F. Wassermann, Phys. Rev. B 72 (2005) 014412.
[56] S.K. Banerjee, Phys. Lett. 12 (1964) 16.
[57] A. Arrott, J.E. Noakes, Phys. Rev. Lett. 19 (1967) 786.
[58] J.S. Kouvel, M.E. Fisher, Phys. Rev. 136 (1964) A1626.